Synthesis and Characterization of Carbon Nanofibers Produced by the Floating Catalyst Method

Charanjeet Singh,* Tom Quested, Chris B. Boothroyd, Paul Thomas, Ian A. Kinloch, Ahmed I. Abou-Kandil, and Alan H. Windle

Department of Materials Science and Metallurgy, University of Cambridge, Pembroke Street, Cambridge CB2 3QZ, United Kingdom

Received: May 22, 2002

A novel method is presented to synthesize herringbone-stacked carbon nanofibers in high selectivity using cobaltocene as the catalytic precursor. Thiophene was essential for carbon nanofiber growth while hydrogen was used as the carrier gas. Selectivity close to 100% was achieved using cobaltocene, thiophene, and hydrogen reacted at 1100 °C. The conversion rate of the nanofibers collected in the cold trap was approximately 1.5 wt % of the initial products. The effect of the catalytic precursor temperature, thiophene, and acetylene was investigated, with reference to nanofiber diameter and selectivity.

Introduction

Carbon nanostructures are becoming of considerable commercial importance with interest growing increasingly rapidly over the decade or so since the discovery of buckminsterfullerene,[1,2] carbon nanotubes,[3–5] and carbon nanofibers.[6–9] There are many methods of producing these nanomaterials, including electric arc discharge,[2–5,10] laser evaporation,[11] chemical vapor deposition (CVD),[6–9,12–15] and plasma-enhanced CVD,[16,17] among many others. Among these, the CVD method seems to be the potential candidate for a commercial-scale process. Indeed, carbon nanofibers as well as multiwalled carbon nanotubes are available currently in large-scale quantities.[15] These nanomaterials have a range of promising properties, including unique mechanical and electrical behavior,[18–20] and are under investigation for a wide range of practical applications such as field emission displays,[21] hydrogen storage,[22,23] nanocomposites,[24,25] and fuel cells.[26,27]

This paper focuses on the synthesis of carbon nanofibers. Carbon nanofibers consist of well-ordered graphite layers, which can be oriented in various directions with respect to the fiber axis. The layers can be parallel, perpendicular, or stacked at an angle to the fiber axis, better known as herringbone arrangement.[26] There are two pathways to synthesize carbon nanofibers by the CVD method. The first involves growing the fibers in the vapor phase, also known as the floating catalyst method,[6,14,28] while the other involves catalysts deposited on supports.[7–9,29,30] Nanofibers are grown through the decomposition of hydrocarbons or carbon monoxide over mono- or bimetallic catalysts, typically Fe, Ni, Co, and Ni–Cu.[7–9,28–33] The formation of carbon nanofibers from the dissociation of acetylene over Fe, Ni, Co, and Cr catalysts was directly observed by in situ transmission electron microscopy (TEM) in the early 70s by Baker.[7,8] The formation of the nanofiber was determined to depend on the diffusion of carbon through the metal catalyst particle. Furthermore, Baker observed an increase in the efficiency of the catalyst when the fibers were grown in hydrogen. For the floating catalyst method, metallocenes are

typically used as a source of the catalyst precursor. Ferrocene has been used extensively, and not much is known about the other types of metallocenes.[6,13,14,28,34] Typically, a desired solution of ferrocene in benzene is sprayed or pumped, or a small amount of ferrocene is sublimed with benzene vapor into a furnace to grow the nanofibers. The reaction is normally done at 1100 °C due to the stability of the hydrocarbon. The role of ferrocene is to provide the iron catalyst, while benzene provides the carbon feedstock required for the nanofiber growth. The addition of sulfur in the form of thiophene has been known to increase the yield of carbon nanofibers.[14,28,30,35–37] Kim showed that low levels of sulfur increased nanofiber yield, while high levels completely suppressed the catalytic activity.[37] The advantage of the floating catalyst method is that it can be a continuous process and therefore be scaled up to produce carbon nanofibers in an industrial scale if the experimental conditions are optimized.

Here, we report the synthesis of herringbone-stacked carbon nanofibers by the floating catalyst method using cobaltocene and ferrocene as the catalytic precursors. Thiophene was essential for carbon nanofiber growth, and hydrogen was used as a carrier gas. Carbon nanofibers were successfully synthesized at selectivity close to 100% under various conditions with a conversion rate of ~1.5 wt %, calculated from the mass of fibers obtained in the cold trap. The effects of the type of catalyst precursor, the precursor temperature, carbon feedstock, and sulfur on nanofiber diameter and composition were investigated.

Experimental Section

Figure 1 shows the experimental setup used to synthesize the carbon nanofibers. Acetylene was used as the carbon feedstock and hydrogen as the carrier gas. Two kinds of catalytic precursors were used, ferrocene and cobaltocene. Both materials have very similar boiling points of around 175 °C. Prior to any runs, the quartz reaction tube (14 mm inner diameter) was heated in an inert argon atmosphere and left for an hour for the temperatures within the furnace to equilibrate. The temperature profile of the first stage furnace had a plateau region in which the catalytic precursors (ferrocene or cobaltocene) were placed. The temperature of this stage of the furnace was referred to as

---

* To whom correspondence should be addressed. Tel: +44 1223 334 335. Fax: +44 1223 334 567. E-mail address: cs266@cam.ac.uk.

10916 *J. Phys. Chem. B, Vol. 106, No. 42, 2002*
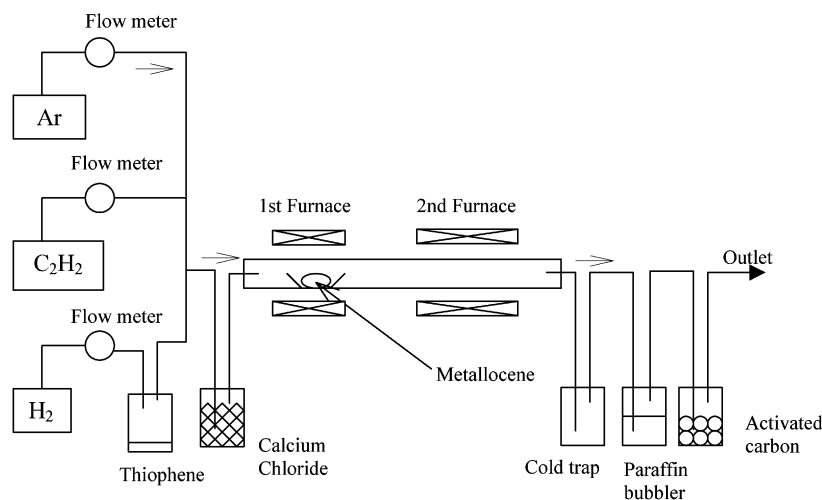
Singh et al.

Figure 1. Schematic of the reactor used for the carbon nanofiber synthesis.

the precursor temperature. Once the temperature had equilibrated, an alumina boat containing 100 mg of the catalytic precursor was placed in the first stage furnace. The argon gas flow was then replaced with hydrogen and acetylene. The hydrogen gas carried the thiophene vapor at a rate determined to be 20 mg min^{-1}. The gases mixed in the drying flask (calcium chloride) before entering the first stage furnace. The second stage furnace temperature was maintained between 1100 and 1150 °C, and the system was operated at ambient pressure. The reaction to form the nanofibers was initiated and completed within this region. The resultant products were deposited in the second stage furnace as well as the cold trap where they were able to settle from the gas stream. Waste gases were passed through paraffin oil and activated carbon balls to remove hydrocarbon and any other toxic byproducts.

The length of the runs was governed by the time it took the deposits to form. The deposits were normally in the form of visible particles suspended in the gas stream. The runs were continued for a further 2 min after deposits had stopped forming to ensure that all of the metallocene supply had been exhausted. If no deposits were formed, the runs were usually stopped after 10 min. Higher precursor temperatures led to shorter runs. The furnaces were turned off and left to cool overnight after each run. A small amount of argon (~10 mL min^{-1}) was left running through the system to prevent oxidation of the nanofibers. The carbon deposits from the cold trap and the outflow end of the quartz tube were collected separately. Deposits from the hot zone of the quartz tube were not collected, as it had been previously observed that these invariably contained large diameter carbon nanofibers.

The variables investigated were the catalyst precursor (metallocene), the catalyst precursor temperature, the flow rate of acetylene, and whether thiophene was present. The hydrogen flow rate was maintained constant at 200 mL min^{-1}. The initial runs were used to determine a relationship between the various parameters and the resulting carbon nanofibers. Next, the effect of the precursor temperature was investigated to see if it had an effect on the size of the catalyst particles and hence the diameter of the nanofibers. Finally, the significance of thiophene and acetylene was studied in the production of carbon nanofibers. These experiments focused on cobaltocene rather than ferrocene, because it had produced high selectivity of nanofibers in the initial runs. The total gas flow was kept approximately constant for all runs, although the ratio of hydrogen to acetylene was varied.

TABLE 1: Conditions for Pyrolysis Runs Forming Experiment 1[a]

run	precursor	thiophene	precursor temp (°C)	H$_2$ flow (mL min^{-1})	C$_2$H$_2$ flow (mL min^{-1})
1	ferrocene	no	180	200[b]	25
2	cobaltocene	no	140	200	50
3	cobaltocene	yes	140	200	50
4	ferrocene	yes	180	200	25
5	cobaltocene	yes	180	200	25

[a] The nanofibers were grown at 1100 °C. [b] Run 1 also had argon (~200 mL min^{-1}) as a carrier gas.

The nanofibers were analyzed using a JEOL 6340 field emission gun scanning electron microscope (FEGSEM), high-resolution TEM (HRTEM) using JEOL 200CX, JEOL 4000EX, and Philips CM300, Renishaw 1000 micro-Raman spectrometer using a 514 nm excitation laser and X-ray diffraction (Cu Kα, $\lambda = 1.54$ Å). Selectivity values were based upon TEM analysis on a number of grid squares examined to ensure that the areas viewed were representative of the sample as a whole. The percentage of selectivity was calculated as a volume fraction of nanofibers to all other forms of carbon deposits, where selectivity (as %) = 100 × (volume of nanotubes/volume of deposit).

Results and Discussion

Effect of Catalyst Precursor (Metallocene). The first five runs were done to establish the relationship between the various parameters and the resulting carbon nanofibers. The experimental conditions for these runs are given in Table 1. SEM images of the products of these runs (Figure 2) reveal that the selectivity of the first four runs consisted of around 10% nanofibers. From SEM and TEM, the nanofibers were heavily coated with amorphous carbon as well as the formation of encapsulated particles. The only run to produce an essentially nanofiber product with high selectivity was run five using cobaltocene, thiophene, a precursor temperature of 180 °C, and 25 mL min^{-1} acetylene. These initial results suggested that cobaltocene seemed to be a better catalyst precursor than ferrocene for this system.

Effect of Catalyst Precursor Temperature. From the initial runs, efforts were concentrated on using cobaltocene as the catalyst precursor and using low flow rates of acetylene (not more than 25 mL min^{-1}). The low flow rate of acetylene was intended to reduce the formation of amorphous carbon through
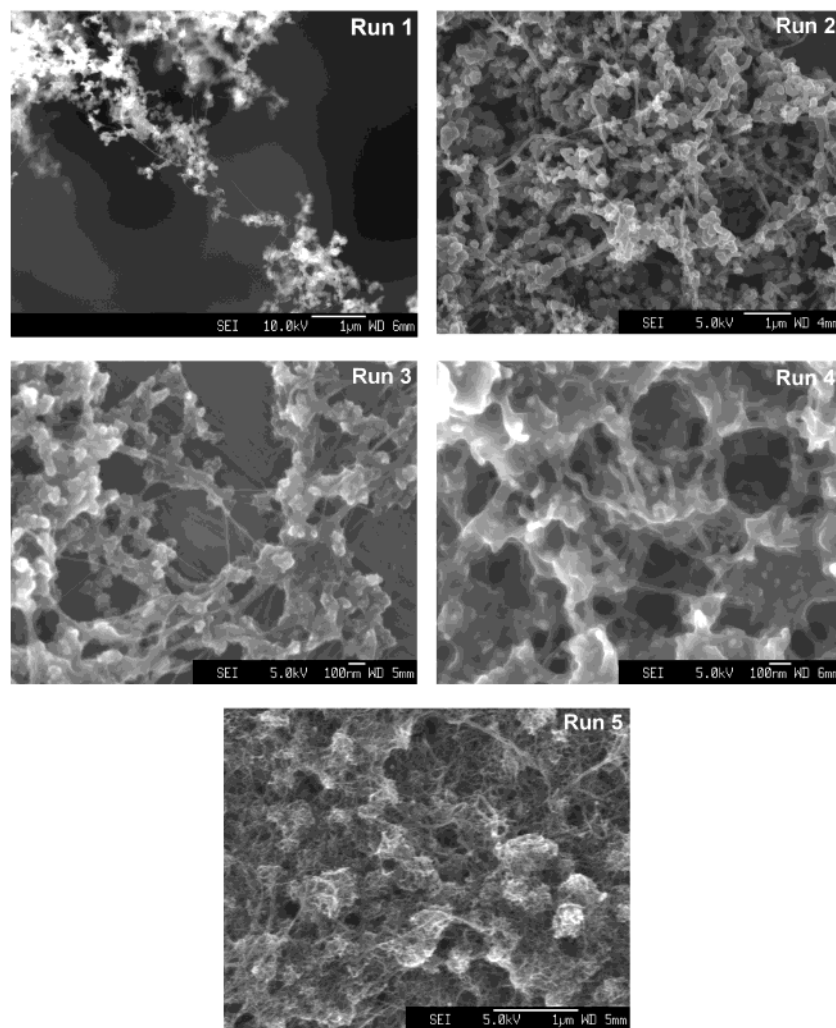
Figure 2. SEM images of the nanofibers formed from initial runs. Runs 1−4 had nanofiber selectivity of around 10%, while run 5 had selectivity of almost 100%. The nanofibers were grown at 1100 °C.

TABLE 2: Effect of Cobaltocene Temperature on the Diameter and Respective Atomic Ratios of the Nanofibers Produced[a]

precursor temp (°C)	mean nanofiber diameter (nm)	atomic ratio, C:Co	atomic ratio, Co:S	atomic ratio, C:S
140	27.2 ± 3.5	302 ± 131.3	0.3 ± 0.12	78.3 ± 13.2
180	14.6 ± 0.6	83.2 ± 5.3	0.5 ± 0.04	42.5 ± 2.5
220	20.8 ± 2.2	22.3 ± 1.7	2.3 ± 0.55	51.4 ± 11.6
250	24.1 ± 5.5	10.3 ± 0.3	3.5 ± 0.31	36.2 ± 3.0

[a] The nanofibers were grown at 1100 °C with a total gas flow rate of 225 mL min^{-1} (200:25 mL min^{-1} H$_2$:C$_2$H$_2$).

thermal decomposition. The effect of the catalyst precursor temperature on the nanofiber diameter and selectivity was then investigated. The flow of hydrogen was kept constant (200 mL min^{-1}), and the acetylene flow was 25 mL min^{-1} with the presence of thiophene. The temperature of the catalyst precursor was varied from 140 to 250 °C. The products obtained were analyzed using energy dispersive X-ray spectroscopy (EDX) and TEM to understand the composition of the cobalt, sulfur, and carbon concentration, as well as nanofiber diameter and selectivity. The results are tabulated in Table 2, while the trends are given in Figure 3. The average diameter of the nanofibers obtained from Figure 3 was typically below 30 nm. The average diameter of the nanofibers obtained was minimized for a temperature around 180 °C, at about 15 nm. This temperature was very similar to the boiling point of cobaltocene, 175 °C. It

may be that the corresponding temperature favors the formation of small clusters of cobalt required for the formation of the nanofibers, therefore producing nanofibers of small diameters.

The ratio of atomic C:Co decreases with increasing catalyst precursor temperature. This can be explained by the fact that more cobaltocene is sublimed with increasing precursor temperature whereas the carbon feedstock from the acetylene and thiophene is held constant, resulting in a decrease of the C:Co ratio. Therefore, the contribution of carbon from the cobaltocene molecule does not have much influence on the C:Co atomic ratio. The Co:S atomic ratio can be explained in a similar manner. The thiophene concentration is not affected by the temperature; therefore, we see an increase in the Co:S ratio with increasing catalyst precursor temperature. The C:S ratio is slightly more difficult to interpret. The higher the catalyst precursor temperature, the higher the amount of cobaltocene sublimed. Cobaltocene is made of one cobalt atom and 10 carbon atoms; therefore, the amount of carbon in the product increases with increasing cobaltocene temperature. The trend seems to indicate that the ratio decreases with increasing temperature, which is opposite to what is expected.

The selectivity of nanofibers from all of these runs is very high and approaches 100% for products collected from the cold trap. SEM images of nanofibers obtained from different precursor temperatures are shown in Figure 4. Figure 4a,b has entangled nanofibers as a result of being sonicated in ethanol,
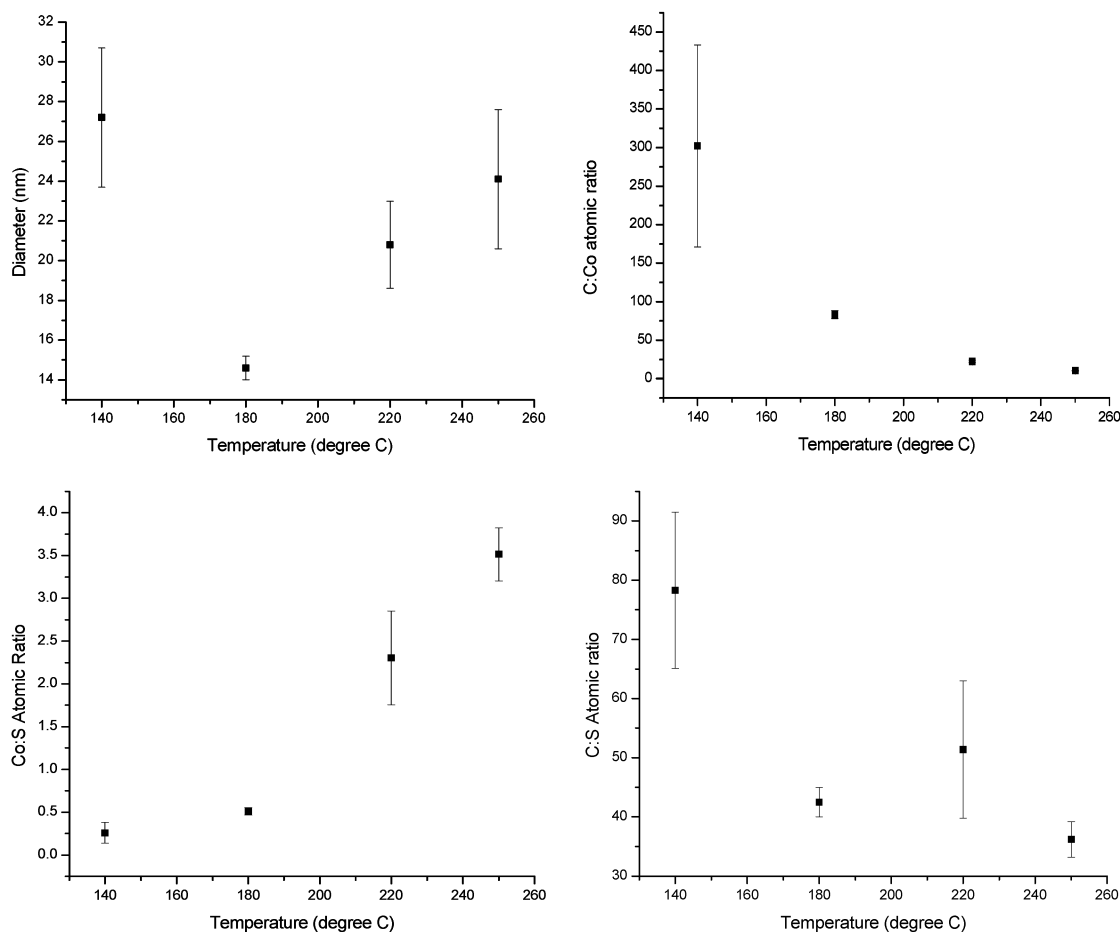
Figure 3. Graphs showing the effect of precursor temperature on the nanofiber diameter, C:Co, Co:S, and C:S atomic ratio.
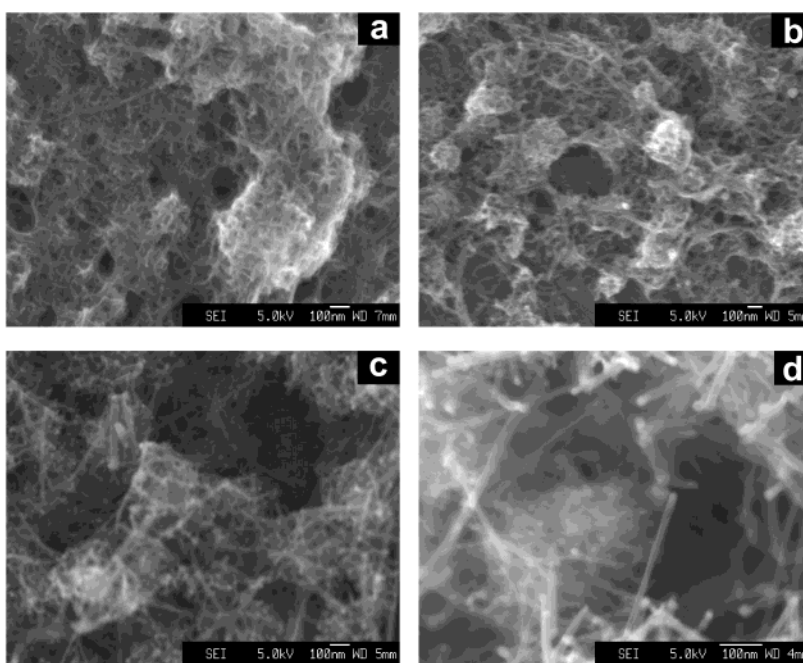

Figure 4. SEM images obtained from different cobaltocene temperatures: (a) 140, (b) 180, (c) 220, and (d) 250 °C. All images indicate a very high selectivity of carbon nanofibers. Almost all of the product is comprised of nanofibers.

while Figure 4c,d has images of the nanofibers as produced. From Figure 4c,d, the fibers are fairly straight and the catalyst particle can be seen attached to the tip. This would indicate that the growth mechanism for the nanofibers is tip growth.

Effect of Acetylene and Thiophene. Prior to these experiments, acetylene was thought as providing the carbon for the nanofiber while thiophene was believed to be the promotor. Several experiments using cobaltocene were conducted to

Synthesis and Characterization of Carbon Nanofibers

J. Phys. Chem. B, Vol. 106, No. 42, 2002 **10919**

TABLE 3: Effect of Acetylene and Thiophene on the Formation of Carbon Nanofibers Obtained from the Cold Trap Using Cobaltocene Heated at 180 °C[a]

| acetylene (mL min^{-1})	thiophene	mean nanofiber diameter (nm)
25	yes	14.6 ± 0.6
0	yes	17.5 ± 1.4
0	no	no deposits formed
25	no	no deposits formed

[a] The nanofibers were grown at 1100 °C, and the total gas flow rate was 225 mL min^{-1}.
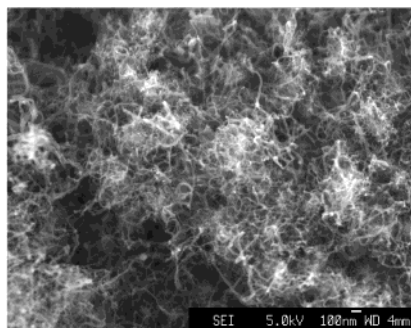
Figure 5. Carbon nanofibers produced without acetylene.
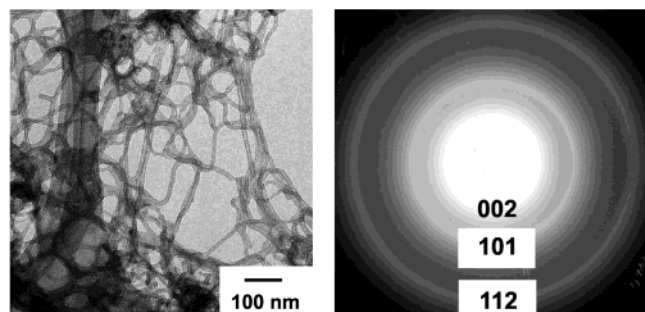
Figure 6. Bright field TEM image of carbon nanofibers as produced. The selectivity and purity of the nanofibers are very high. On the right is a diffraction pattern taken from the same area of the nanofibers. The nanofibers were grown at 1100 °C using cobaltocene heated at 180 °C, thiophene, and a total gas flow rate of 225 mL min^{-1} (200:25 mL min^{-1} H$_2$:C$_2$H$_2$).

understand the role of acetylene and thiophene. The total flow rates of the gases were kept constant (225 mL min^{-1}) while the catalyst precursor temperature was kept constant at 180 °C.

Table 3 lists the results obtained from these experiments. An interesting observation was that the nanofibers could be formed in the cold trap even without the presence of acetylene but not without thiophene. Figure 5 shows a SEM image of the nanofibers obtained without acetylene. The amount of carbon from cobaltocene and thiophene was calculated to be 6.4 and 11.4 mg min^{-1}, respectively. Therefore, thiophene is the main source of carbon for the nanofiber formation. Another interesting point to note is that the nanofiber diameter has slightly increased. Without thiophene, no nanofiber deposits were formed in the cold trap.

Characterization of Carbon Nanofibers. To determine the nanoscale structure of the nanofibers, all of the samples were examined by TEM. Figure 6 shows one example of a low magnification bright field image and a diffraction pattern of the carbon nanofibers produced during run five, using both cobaltocene and thiophene. Apart from the carbon support film, only nanofibers are visible in the image, indicating that the selectivity and purity of the nanofibers are very high. The diffraction pattern was taken from the same area as the image. The presence of rings in the diffraction pattern, rather than
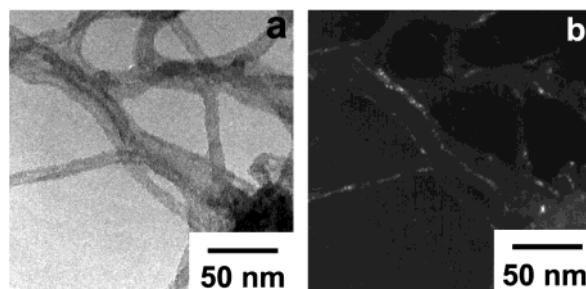
Figure 7. TEM images showing (a) bright field image of carbon nanofibers and (b) dark field image of carbon nanofibers with the objective aperture on the 002 ring. Analysis of the dark field image indicates that carbon fibers have a herringbone structure. The nanofibers were grown at 1100 °C using cobaltocene heated at 180 °C, thiophene, and a total gas flow rate of 225 mL min^{-1} (200:25 mL min^{-1} H$_2$:C$_2$H$_2$).
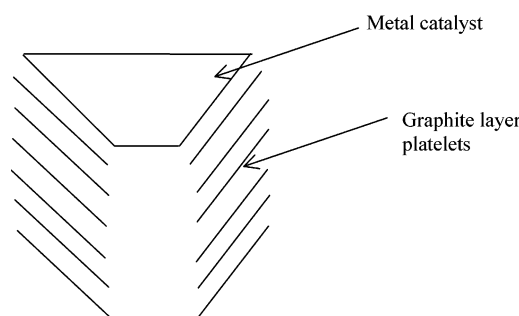
Figure 8. Schematic showing a cross-section herringbone carbon nanofiber with a metal catalyst and the graphite layers.

discrete spots, is because the crystal planes have many orientations. Because the crystal planes all have the same orientation in each fiber, the presence of rings means that the fibers are randomly orientated.

A higher magnification bright field image of the same sample is shown in Figure 7a. This shows that some of these nanofibers have hollow cores. Figure 7b shows a dark field image of the same area as panel a. The dark field image was taken with the beam tilted so that part of the graphite 002 ring passes through the objective aperture. Comparison of Figure 7b with the bright field image, Figure 7a, shows that only one side of each fiber is bright. This means that for these fibers, the graphite 002 lattice planes are correctly oriented to diffract into the objective aperture on only one side of the fiber. Figure 7b therefore verifies that the nanofibers have a herringbone structure, where the graphite 002 lattice planes are inclined to the axis of the fiber, as shown schematically in Figure 8.

The herringbone structure of these nanofibers is confirmed in the high-resolution images shown in Figure 9. Figure 9a shows the graphite 002 planes in a single nanofiber, from which it can be seen that the 002 planes are inclined at between 30 and 40° to the fiber axis. Figure 9b shows the tip of a nanofiber containing a catalyst particle. It can be seen that the 002 planes are parallel to the surface of the catalyst particle, suggesting that the angle between the 002 planes and the fiber axis is determined by the shape of the catalyst particle, as proposed by Boellard.[29]

Herringbone nanofibers such as those shown in Figure 7 were produced in all of the runs where cobaltocene and thiophene were present. When thiophene was absent, no deposits were obtained in the cold trap. Instead, nanofibers with layers parallel to the fiber axis, in selectivity of less than 10%, were obtained from the outflow end of the reaction tube, suggesting that sulfur plays an important role in the formation of herringbone
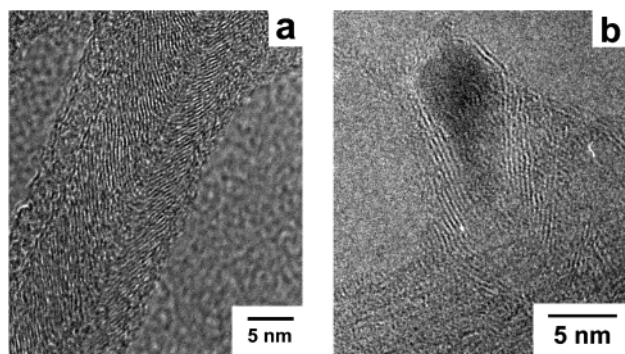
Figure 9. High-resolution 002 lattice images taken from (a) cross-section of carbon nanofiber covered by a layer of amorphous carbon and (b) catalyst particle. HRTEM images confirm the herringbone structure arrangement. The nanofibers were grown at 1100 °C using cobaltocene heated at 140 °C and with a total gas flow rate of 250 mL min^{-1} (200:50 mL min^{-1} H$_2$:C$_2$H$_2$).
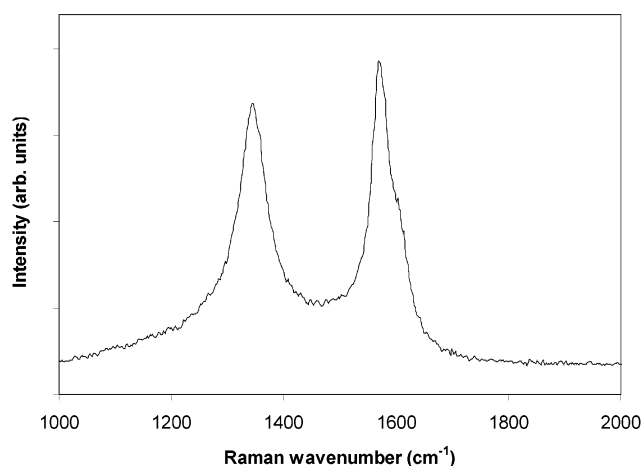

Figure 10. Raman spectrum taken from carbon nanofiber using an argon 514 nm excitation laser. The spectrum was taken from nanofibers grown at 1100 °C using cobaltocene heated at 220 °C, thiophene, and a total gas flow rate of 225 mL min^{-1} (200:25 mL min^{-1} H$_2$:C$_2$H$_2$).

nanofibers. With a ferrocene precursor, very few nanofibers were produced.

Raman spectroscopy was also done on the nanofibers. The Raman spectrum was taken using a 514 nm Argon laser excitation wavelength. The first order Raman spectrum typically between 1000 and 1800 cm^{-1} is composed of two main peaks, at around 1350 and 1580 cm^{-1}. The former corresponds to the defect-induced Raman band and is known as the defect mode, A$_{1g}$ or D peak, while the latter corresponds to the Raman-allowed E$_{2g2}$ mode, also known as the G peak. Also within the spectrum, the G peak has a shoulder known as the D′ peak at around 1620 cm^{-1}. This peak is due to the maximum in the phonon density of states. The D and D′ peaks correlate with the size of the crystal, i.e., a smaller crystal would give rise to a larger peak.[38,39] An example of a Raman first-order spectrum taken of the nanofibers is given in Figure 10. From this, it can be seen that the D and D′ peaks are quite large, indicating that the crystal size within the nanofibers is small. This is verified by the TEM image shown in Figure 9.

X-ray powder diffraction (XRD) was also done on the nanofibers, and the pattern scan is given in Figure 11. The XRD pattern reveals graphite like peaks in the sample. The graphite (002), (004), and (110) reflections are distinct at 26, 54, and 77°. The cobalt (111), (200), (220), (311), and (222) are also present and correspond to 44.3, 51.5, 76, 92.4, and 97.7°. Several other peaks are present at 29.9 and 31.3°. These peaks were
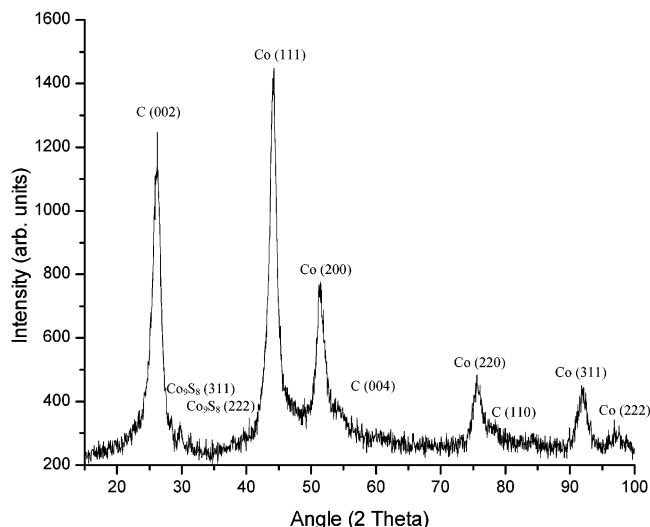

Figure 11. X-ray diffraction pattern taken from the carbon nanofibers produced. The pattern was taken from nanofibers grown at 1100 °C using cobaltocene heated at 220 °C, thiophene, and a total gas flow rate of 225 mL min^{-1} (200:25 mL min^{-1} H$_2$:C$_2$H$_2$).

found to correspond to cobalt sulfide, Co$_9$S$_8$. Therefore, the catalyst is composed mainly of cobalt particles with some cobalt sulfide particles. There is a possibility that the sulfur in the thiophene had reacted with the cobaltocene to form this sulfide, which might favor the growth of carbon nanofibers in the vapor phase. Furthermore, herringbone structures are believe to form when the catalyst particle is made of an alloy.[40,41]

The results obtained using energy-filtered TEM (EFTEM) are consistent with those achieved by X-ray analysis. EFTEM has been shown to be an efficient tool for the acquisition of species sensitive chemical distribution maps.[42] The analysis was performed using a Philips CM300 FEG-TEM equipped with a Gatan imaging filter (GIF). The zero-loss (or elastic-scattering) image in Figure 12 shows nanofibers deposited onto holey carbon films. The catalyst particles can be seen attached to some of these nanofibers. By recording a series of energy-filtered images over a large energy loss range, it is possible to map out the location of each element present.[43] The location of cobalt and sulfur can be seen originating from the catalyst areas, while the nanofiber and the carbon grid consist solely of carbon. The EFTEM analysis indicates that the particle is a cobalt sulfide alloy, consistent with the findings of the X-ray analysis. Hence, this technique has confirmed the presence of sulfur in the nanoparticles, which is believed to play an important role with the cobalt in the production of these nanofibers in the vapor phase.

Growth Mechanism. Here, we propose the growth mechanism involved in producing these nanofibers in the vapor phase. The sublimed cobaltocene together with the acetylene, hydrogen, and thiophene vapor enter the second stage furnace maintained at 1100 °C. The cobaltocene decomposes and forms clusters of cobalt particles, which reacts with the thiophene to form cobalt sulfide clusters, which are appropriate for nanofiber synthesis. This is supported by Kim who demonstrated that low levels of H$_2$S (4−100 ppm) in cobalt can dramatically enhance the formation of nanofibers, while with high levels (>500 ppm), the catalytic action is suppressed.[37] It was suggested that the enhancement of carbon deposition is related to the reconstruction of the metal surface coupled with the blocking action of the sulfur atoms toward the formation of a graphitic overlayer. A similar behavior such as that observed by Kim is thought to occur in the current system. The hydrogen carrier gas reacts
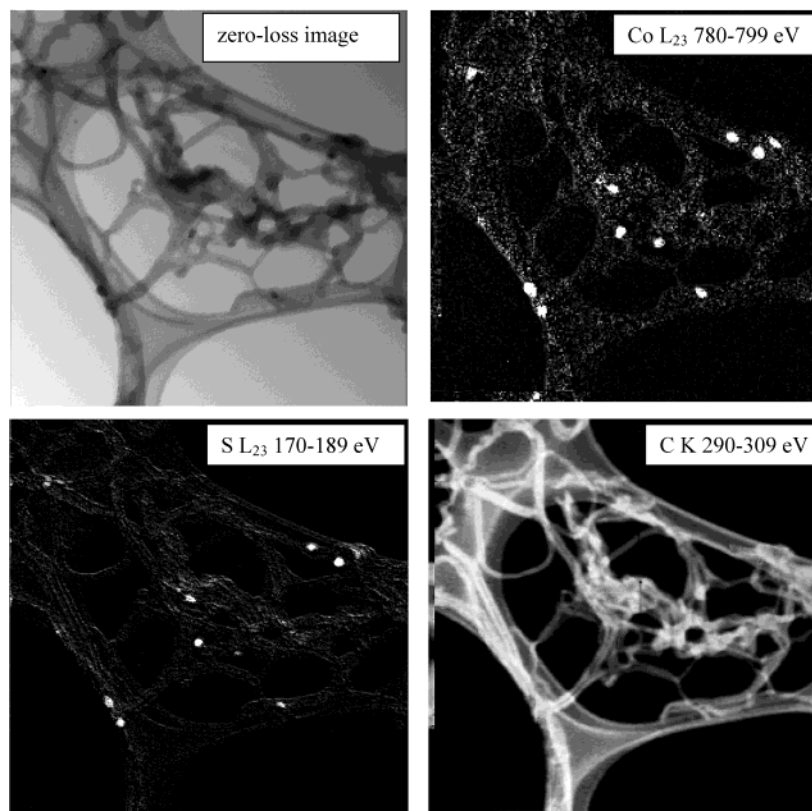
Synthesis and Characterization of Carbon Nanofibers

J. Phys. Chem. B, Vol. 106, No. 42, 2002 **10921**

Figure 12. EFTEM analysis conducted on carbon nanofibers. The zero-loss image shows nanofibers with catalyst particles attached to some of these nanofibers. The three elemental maps for Co, S, and C were obtained by collecting an image using electrons in a 19 eV energy loss range just after the edge of interest and then subtracting a background calculated from two images taken with a lower energy loss. The analysis indicates the presence of cobalt (Co L_{23}, energy range 780−799 eV) and sulfur (S L_{23}, energy range 170−189 eV) at the catalyst particles. The nanofibers were grown at 1100 °C using cobaltocene heated at 180 °C, thiophene, and a total gas flow rate of 225 mL min^{-1} (200:25 mL min^{-1} H_2:C_2H_2).

with the sulfur to form H_2S at elevated temperatures. The H_2S will then react with the cobalt clusters to form the sulfide compound. This process occurs rapidly since the growth time of the nanofibers in the heated zone was calculated to be between 4 and 5 s.

The growth mechanism of the nanofibers from the catalyst particles is similar to that proposed by Baker, even though the reaction conditions are different.[7] The thiophene and acetylene arrive at the catalyst particle and dissociate to form atomic carbon species and then dissolve into the catalyst particle, diffuse to the end, and precipitate to form graphite layers. The arrangement of these layers would depend on the shape of the catalyst particle where it precipitates. From Figure 4d, the catalyst is seen to be at the tip of the nanofiber. This suggests that the nanofiber is growing by the tip growth mechanism. The presence of thiophene is crucial for the nanofibers to grow in the vapor phase and form herringbone structures. Figure 13 shows the SEM image of the as grown nanofibers, which are growing in the vapor phase. The nanofibers can be seen to form in aggregates or balls less than 1 μm in diameter with fibers pointing out. It's evident that the nanofibers are growing in the vapor phase and in the process are getting entangled to form these aggregates.

Conclusions

A novel method is presented to synthesize herringbone-stacked carbon nanofibers in the vapor phase in high selectivity using cobaltocene as the catalytic precursor with the presence of thiophene. From the study done, cobaltocene seems to be more efficient as a catalyst precursor than ferrocene to synthesize herringbone carbon nanofibers for this system. The nanofibers
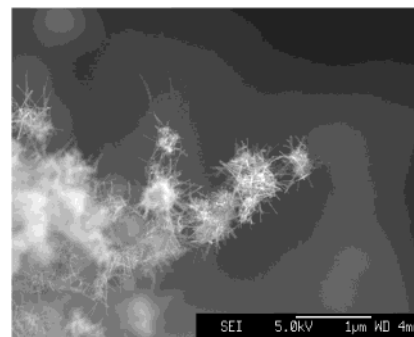

Figure 13. Carbon nanofibers collected in the cold trap. The nanofibers seem to be pointing outward from circular aggregates. The nanofibers were grown at 1100 °C using cobaltocene heated at 250 °C, thiophene, and a total gas flow rate of 225 mL min^{-1} (200:25 mL min^{-1} H_2:C_2H_2).

have a minimum average diameter of around 15 nm when the precursor temperature is 180 °C, which corresponds to the boiling point of cobaltocene. This is most probably due to the formation of small clusters of catalytic particles for the nanofiber growth. Furthermore, the formation of nanofibers required thiophene and not acetylene as the carbon feedstock. The sulfur from the thiophene reacts with the cobalt particles to form a sulfide and promotes the carbon nanofiber growth in the vapor phase with hydrogen as the carrier gas. Selectivity close to 100% under various conditions was successfully achieved with conversion rates as high as ~1.5 wt %. The advantage of this process is that it can be scaled up for large-scale production. These nanofibers may have potential application as field emitters, gas storage, and composites.[9,22]

References and Notes

(1) Kroto, H. W.; Heath, J. R.; Obrien, S. C.; Curl, R. F.; Smalley, R. E. *Nature* **1985**, *318*, 162.

(2) Kratschmer, W.; Lamb, L. D.; Fostiropoulos, K.; Huffman, D. R. *Nature* **1990**, *347*, 354.

(3) Iijima, S. *Nature* **1991**, *354*, 56.

(4) Iijima, S.; Ichihashi, T. *Nature* **1993**, *363*, 603.

(5) Bethune, D. S.; Kiang, C. H.; Devries, M. S.; Gorman, G.; Savoy, R.; Vazquez, J.; Beyers, R. *Nature* **1993**, *363*, 605.

(6) Endo, M. *Chemtech* **1988**, *18*, 568.

(7) Baker, R. T. K.; Barber, M. A.; Harris, P. S.; Feates, F. S.; Waite R. J. *J. Catal.* **1972**, *26*, 51.

(8) Baker, R. T. K.; Harris, P. S.; Thomas, R. B.; Waite, R. J. *J. Catal.* **1973**, *30*, 86.

(9) Terrones, H.; Hayashi, T.; Munoz-Navia, M.; Terrones, M.; Kim, Y. A.; Grobert, N.; Kamalakaran, R.; Dorantes-Davila, J.; Escudero, R.; Dresselhaus, M. S.; Endo, M. *Chem. Phys. Lett*, **2001**, *343*, 241.

(10) Ebbesen, T. W.; Ajayan, P. M. *Nature* **1992**, *358*, 220.

(11) Thess, A.; Lee, R.; Nikolaev, P.; Dai, H. J.; Petit, P.; Robert, J.; Xu, C. H.; Lee, Y. H.; Kim, S. G.; Rinzler, A. G.; Colbert, D. T.; Scuseria, G. E.; Tomanek, D.; Fischer, J. E.; Smalley, R. E. *Science* **1996**, *273*, 483.

(12) Joseyacaman, M.; Mikiyoshida, M.; Rendon, L.; Santiesteban, J. G. *Appl. Phys. Lett.* **1993**, *62*, 657.

(13) Endo, M.; Takeuchi, K.; Kobori, K.; Takahashi, K.; Kroto, H. W.; Sarkar, A. *Carbon* **1995**, *33*, 873.

(14) Kato, T.; Kusakabe, K.; Morooka, S. *J. Mater. Sci. Lett.* **1992**, *11*, 674.

(15) Tennent, H. G.; Barber, J. J.; Hoch, R. U. S. Patent 5,578,543, 1996.

(16) Ren, Z. F.; Huang, Z. P.; Xu, J. W.; Wang, J. H.; Bush, P.; Siegal, M. P.; Provencio, P. N. *Science* **1998**, *282*, 1105.

(17) Merkulov, V. I.; Lowndes, D. H.; Wei, Y. Y.; Eres, G.; Voelkl, E. *Appl. Phys. Lett.* **2000**, *76*, 3555.

(18) Treacy, M. M. J.; Ebbesen, T. W.; Gibson, J. M. *Nature* **1996**, *381*, 678.

(19) Wong, E. W.; Sheehan, P. E.; Lieber, C. M. *Science* **1997**, *277*, 1971.

(20) Frank, S.; Poncharal, P.; Wang, Z. L.; de Heer, W. A. *Science* **1998**, *280*, 1744.

(21) Lee, C. J.; Lee, T. J.; Park, J. *Chem. Phys. Lett.* **2001**, *340*, 413.

(22) Chambers, A.; Park, C.; Baker, R. T. K.; Rodriguez, N. M. *J. Phys. Chem. B* **1998**, *102*, 4253.

(23) Park, C.; Anderson, P. E.; Chambers, A.; Tan, C. D.; Hidalgo, R.; Rodriguez, N. M. *J. Phys. Chem. B* **1999**, *103*, 10572.

(24) Andrews, R.; Jacques, D.; Rao, A. M.; Rantell, T.; Derbyshire, F.; Chen, Y.; Chen, J.; Haddon, R. C. *Appl. Phys. Lett.* **1999**, *75*, 1329.

(25) Sandler, J.; Shaffer, M. S. P.; Prasse, T.; Bauhofer, W.; Schulte, K.; Windle, A. H. *Polymer* **1999**, *40*, 5967.

(26) Bessel, C. A.; Laubernds, K.; Rodriguez, N. M.; Baker, R. T. K. *J. Phys. Chem. B* **1998**, *102*, 1115.

(27) Steigerwalt, E. S.; Deluga, G. A.; Cliffel, D. E.; Lukehart, C. M. *J. Phys. Chem. B* **2001**, *105*, 8097.

(28) Ci, L. J.; Li, Y. H.; Wei, B. Q.; Liang, J.; Xu, C. L.; Wu, D. H. *Carbon* **2000**, *38*, 1933.

(29) Boellaard, E.; De Bokx, P. K. *J. Catal.* **1985**, *96*, 481.

(30) Rodriguez, N. M. *J. Mater. Res.* **1993**, *8*, 3233.

(31) Rodriguez, N. M.; Kim, M. S.; Baker, R. T. K. *J. Catal.* **1993**, *144*, 93.

(32) Rodriguez, N. M.; Kim, M. S.; Baker, R. T. K. *J. Catal.* **1993**, *140*, 16.

(33) Krishnankutty, N.; Rodriguez, N. M.; Baker, R. T. K. *J. Catal.* **1996**, *158*, 217.

(34) Ci, L. J.; Wei, J. Q.; Wei, B. Q.; Liang, J.; Xu, C. L.; Wu, D. H. *Carbon* **2001**, *39*, 329.

(35) Vander Wal, R. L.; Ticich, T. M.; Curtis, V. E. *J. Phys. Chem. B* **2000**, *104*, 11606.

(36) Ishioka, M.; Okada, T.; Matsubara, K. *Carbon* **1992**, *30*, 865.

(37) Kim, M. S.; Rodriguez, N. M.; Baker, R. T. K. *J. Catal.* **1993**, *143*, 449.

(38) Tunistra, F.; Koenig, J. L. *J. Chem. Phys.* **1970**, *53*, 1126.

(39) Endo, M.; Nishimura, K.; Kim, Y. A.; Hakamada, K.; Matushita, T.; Dresselhaus, M. S.; Dresselhaus, G. *J. Mater. Res.* **1999**, *14*, 4474.

(40) Kim, M. S.; Rodriguez, N. M.; Baker, R. T. K. *J. Catal.* **1992**, *134*, 253.

(41) Park, C.; Engel, E. S.; Crowe, A.; Gilbert, T. R.; Rodriguez, N. M. *Langmuir* **2000**, *16*, 8050.

(42) Reimer, L. *Mater. Trans*. **1998**, *39*, 873.

(43) Thomas, P. J.; Midgley, P. A. *Ultramicroscopy* **2001**, *88*, 179.